Reynolds number effects on VIV of a splitter plate

Tero Pärssinen, Hannu Eloranta, Pentti Saarenrinne

Energy and Process Engineering, Tampere University of Technology, Tampere, Finland, tero.parssinen@tut.fi

Abstract The development of Vortex-Induced Vibration (VIV) with increasing Reynolds number in the wake of a splitter plate has been examined with Particle Image Velocimetry (PIV) and High-Speed Digital Imaging (HSDI). Previous studies e.g. Eloranta et al. (2005) have shown that flow separation from the trailing edge of a splitter plate in a convergent channel involves fluid-structure interactions, modifying the fundamental instability related to vortex shedding. Under certain conditions, the VIV induces cellular vortex shedding from the trailing edge. This paper reports measurements of the effects of Reynolds number on plate vibration and the resulting effects on the flow. The objective of this work was to gain more information on the Reynolds number dependency of the VIV system. Experimental work includes HSDI measurements to assess the vibrational response of the plate and PIV measurements to study the effect of vibration to the flow field. Combining data from these techniques, the development of the vibration frequency can be addressed together with the imprint of the vibration mode in the flow. The results show that over most of the Reynolds numbers measured, the plate vibrates in a distinct mode characterized by a spanwise standing wave along the plate trailing edge. The vibration frequency and the spacing between the nodes of the standing wave depend on the Reynolds number. As the Reynolds number is increased, the frequency of the dominant vibration mode does not increase linearly, but in a stepwise fashion. The plot of vibration frequency as a function of Reynolds number shows that the vibration frequency of the VIV system tends to lock-in to a rather constant value i.e. to a natural frequency of the system, over a range of Reynolds numbers. After certain Reynolds number threshold is exceeded the frequency jumps to a new level.

1. Introduction

Flow separation from the trailing edge of a splitter plate in a convergent channel involves intricate fluid dynamics including fluid-structure interaction (FSI), or more specifically vortex-induced vibration (VIV). Eloranta et al. (2004 & 2005) showed that under certain conditions the fundamental instability related to vortex shedding from the trailing-edge is modified by the VIV and cellular shedding of spanwise vorticity is observed. The build up of the cellular structure is a result of fluid – structure interaction, in which three-dimensional modes of the plate vibration establish a standing wave along the plate trailing edge. Vortex shedding occurs in cells separated by nodes of the standing wave.

To the best of the authors' knowledge, studies on the physics of VIV of a splitter plate at high Reynolds number are not reported in the open literature. However, some examples of rather similar studies with different objectives can be found. The aeroelasticity of flat plates has received some attention. For example, Yamaguchi et al. (2000a and 2000b) studied flutter properties of thin plates in high speed flows. They developed a model for the prediction of flutter and performed experiments on the flutter onset and mode for sheets made of different materials. Vortex shedding from circular cylinders and vibrations thereof are well documented in the literature. As presented earlier, the cellular shedding in the present case is a consequence of the vibration mode of the plate. Similar type of vibration is observed for flexible cables or beams in cross-flow; see e.g. Newman and Karniadakis (1996), Evangelinos and Karniadakis (1999) or Willden and Graham (2004). Like in the present setup, vortex shedding from the cable creates fluctuating force to the structure and induces vibration. Depending on the end conditions, structural properties and Reynolds number, a standing wave vibration mode may be build up along the cable. The results presented earlier

describe the organization of vortex shedding and structure of the wake following from the cellular shedding. This data from the flow shows qualitative similarity with literature concerning wakes of vibrating cables. Other typical cases to produce cellular shedding are those of rigid cylinders placed in spanwise shear flow and spanwise tapered bodies placed in homogeneous flow (see e.g. Lucor et al. 2001 and Castro & Rogers 2002). In these cases the spanwise variation of preferred shedding frequency forces static cells with different shedding frequencies to form along the span of a cylinder.

The experiments are conducted in a 2D convergent channel with a rectangular cross-section. The stiff polycarbonate splitter plate is mounted in the middle of the channel inlet. The other end is free to move according to flow. The motivation to this study arises from a nozzle design in which the splitter plate is used to divide two streams and three-dimensional secondary flows arising at the trailing edge should be avoided to ensure controlled mixing. Besides the quality issues also structural durability need to be considered at the design stage if high amplitude vibrations are expected.

The effect of Reynolds number to the response of the combined splitter plate – flow system is studied by changing the flow rate in the channel. The frequency of plate vibration is measured by high-speed digital imaging (HSDI) as a function of the Reynolds number. The aim is to show how the flow rate modifies the VIV and determines the vibration frequency. PIV is used to study the corresponding effect of the vibration mode to the flow.

The paper starts by presenting the experimental setup and measurements in section 2. Since the experimental procedures and background for conventional PIV are well known it will be repeated here only briefly. The analysis technique for HSDI data is introduced in section 3. The results in section 4 start with illustrating the mode of vibration. After this, a general response of the plate as a function of Reynolds number is presented. The conclusions are made in section 5. More detailed results, observations and discussion will be published in Eloranta et al. (2006).

2. Experimental set-up and data acquisition

The measurements are carried out in a 2D convergent channel with a rectangular cross-section. Important dimensions, normalized by the trailing-edge thickness (h = 1mm), are presented in Fig. 1. Width of the channel is 120h. The length of the splitter plate is 600h with the last 50h of the plate tapered from the body thickness of 3h to 1h in the trailing edge. The plate is hinged from the

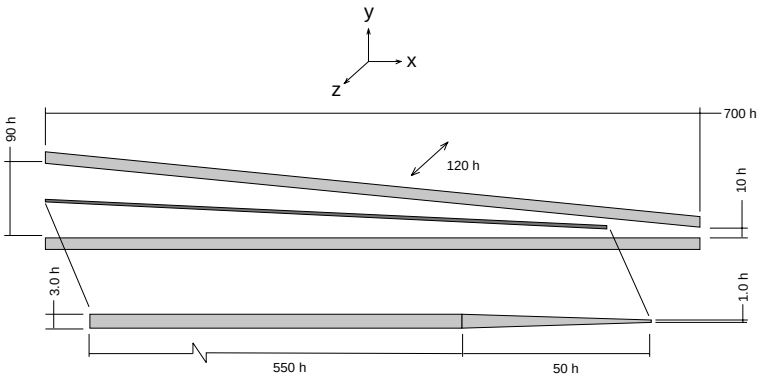

Fig. 1. Dimensions of the flow channel and the splitter plate.

upstream end, while the other end is free to move according to flow. The material of the plate is polycarbonate with following properties taken from literature: Young modulus E = 2200MPa, Poisson ratio ν = 0.375, and density ρ = 1200kg/m^3. The convergent channel is installed into a water loop fed by a centrifugal pump. The Reynolds numbers, based on the trailing-edge thickness h and the free-stream velocity U_E at the trailing-edge are presented in the results section. The coordinate system is also presented in the Fig. 1.

PIV (2D-2C) measurements are performed just after the trailing edge in the *x*-*z* -plane. A measurement window with dimensions of 60x30h^2 (*x*-*z*) is used and vectors are computed to a grid with the size of 80x40 nodes. This results in a spatial resolution of approx. 0.8*h*, which is the spacing between two adjacent vectors. PIV data is obtained at the wake symmetry line 20*h* after the trailing-edge. The location of the PIV measurement plane is presented in Fig. 2. In the *x*-*y* –plane HSDI measurements are conducted. In this plane the measurement window is considerably smaller covering only a narrow area of the plate tip. HSDI is used to investigate the vibration of the plate. The measurement area is fixed in *z*-direction thus the comparison of vibration amplitude at different Reynolds numbers is not feasible as some measurements may coincide with a node area at that Re number and some an anti-node area with different Re number. HSDI measurement position is also indicated in Fig. 2. The sampling rate used in the measurements is 6 kHz and the number of samples is 2000. Image analysis is used to extract the tip *y*-position. The analysis is based on detecting the surface contour in each frame. The PIV and HSDI systems are introduced in Tables 1 and 2. Both systems are operated with LaVision PTU8 control unit and DaVis software.

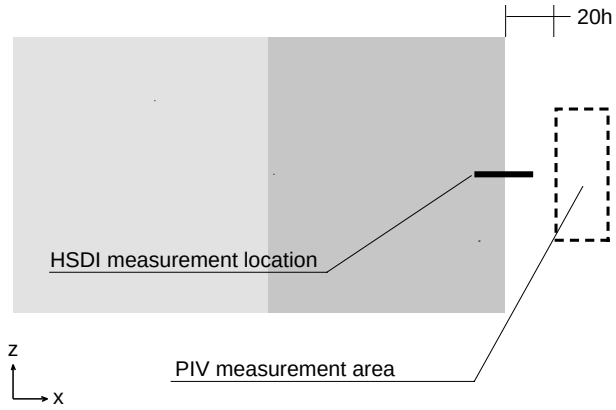

Fig. 2. PIV (dashed) and HSDI (solid) measurement positions in the *x*-*y* and *x*-*z* –planes.

Table 1. Conventional PIV system.

CAMERA	FlowMaster3 (PCO Sensicam double-frame)	
	resolution	1280x1024 pixels
	pixel size	6.4x6.4 microns
	dynamics	12bit
	image rate	10Hz (4Hz double-frame) @ full-frame
LASER	Double-cavity Nd:YAG laser (Spectra-Physics)	
	pulse energy	400mJ
	pulse duration	5ns
	pulse rate	4Hz

Table 2. Time-resolved PIV system.

CAMERA	ImagerPro HS (PCO 1200HS)	
	resolution	1280x1024 pixels
	pixel size	12x12 microns
	dynamics	10bit
	image rate	634Hz @ full-frame
LASER	Double-cavity Nd:YLF laser (New Wave Pegasus PIV)	
	pulse energy	10mJ
	pulse duration	40ns
	pulse rate	20kHz

3. HSDI data analysis

Next the analysis technique for the HSDI data is presented. In our previous paper (e.g. Eloranta, 2004), PIV system was used to track the tip movement by image analysis. Now, HSDI system will be used to perform similar experiments with higher time-resolution enabling spectral analysis. HSDI is used to map the development of the vibration frequency over a wide range of Reynolds numbers. PIV is used to measure conventional fluid properties from the wake. With both techniques, totally 49 flow rates are measured. The flow rate is increased with small steps and similar set of experiments is conducted for each step. The flow rate is characterized by Reynolds number, which is based on free-stream velocity U_E at the plate tip and trailing-edge thickness h. The Reynolds numbers, corresponding to each measured case, are given in the results section.

The system is based on Nd-YFL laser (New Wave Pegasus-PIV) with sheet optics and high-speed 1Mpix CMOS camera (LaVision Imager Pro HS), presented in Table 2. This system can be operated at a maximum of 10 kHz framing rate with a single-frame mode. With this equipment, theoretically vibration frequencies up to 5 kHz can be detected. Now, the system is operated at 6 kHz framing rate enabling the detection of vibration frequencies up to 3 kHz.

The field of view is limited to cover only the plate tip. The laser sheet, aligned normal to plate surface, illuminates the surface contour. The measurement position is located in the mid-span of the plate trailing edge, as indicated in Fig 2. Image analysis technique analogous to that explained in the earlier papers (Eloranta et al. 2005) is used to extract the tip y-position in each frame. Shortly, the image is first filtered and convoluted with a line mask and then a vertical intensity profile is extracted. The intensity profile is differentiated and then maximum derivative is located with an accuracy of one pixel. Sub-pixel accuracy is achieved by a polynomial fit to three points around the maximum. An example of a time-trace of the tip movement is presented in Fig. 3. This vibration has a frequency and peak-to-peak amplitude of approx. 1680Hz and 80μm, respectively. Clearly a trace of low frequency (< 100 Hz) modulation from the vibration of the whole measurement system is also observed. The time-trace of the tip y-position is input to spectral estimation in order to get the frequency of the vibration. In the experiments, 2000 images of the plate tip are collected at each Reynolds number and the position data is analyzed by a Fast-Fourier Transform algorithm (*FFT*). The length of the FFT is 1024 units, the signal is divided into eight sections, and 50% overlapping is used in the spectral estimation, based on the Welch method (Welch, 1967).

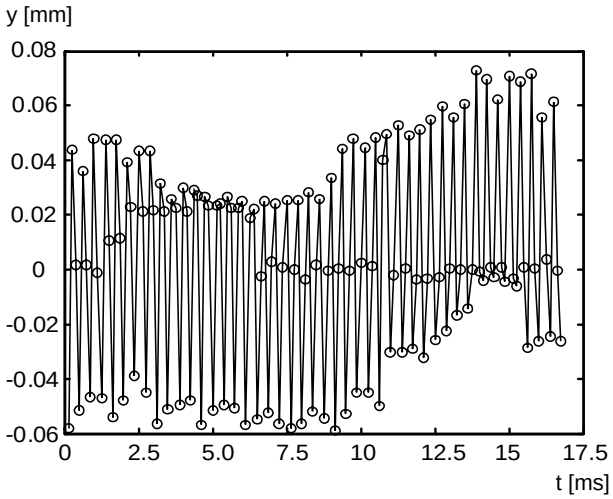

Fig. 3. An example of the time-trace of the tip *y*-position detected by HSDI.

For an estimate of the accuracy of the tip detection one would need to measure a splitter plate that does not vibrate. This is not feasible at these flow velocities. As an approximate we measured a stainless steel splitter plate with thick trailing-edge. This plate has very low vibration amplitudes over most of our Reynolds number range. Figure 4 presents a time-trace of the tip movement measured with the stainless steel plate at Re = 5400. The corresponding plate vibration frequency is approx. 2 kHz. The plot shows a rather periodical vibration with amplitude less than 2 μm. As the HSDI system is able to detect vibration amplitudes in the range of few microns it is deduced that the vibration of the polycarbonate plate with amplitudes usually exceeding 30 microns can be reliably measured.

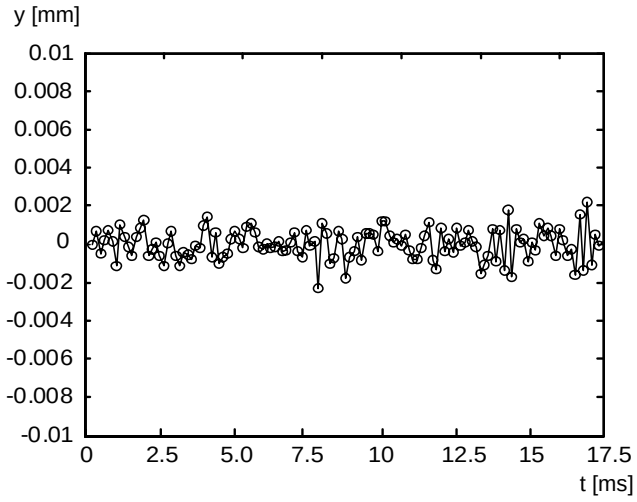

Fig. 4. An example of the time-trace of low amplitude vibration with stainless steel plate.

4. Results

In the following chapter we present results providing information on the Reynolds number dependency of the VIV system. In our earlier experiments e.g. Eloranta et al. (2005) we have verified that VIV induces a standing wave vibration mode at the trailing edge of the plate leading to locked-in vortex shedding and a periodic pattern in the mean flow field. Figure 5 presents a

snapshot from computational modal analysis displaying a typical standing vibration mode. Streamwise direction is indicated with a red arrow. The amplitude of the vibration at the tip is enlarged for better observation. One can quite easily see how the standing wave can amplify the vortex shedding and induce a streaky pattern in the mean flow field.

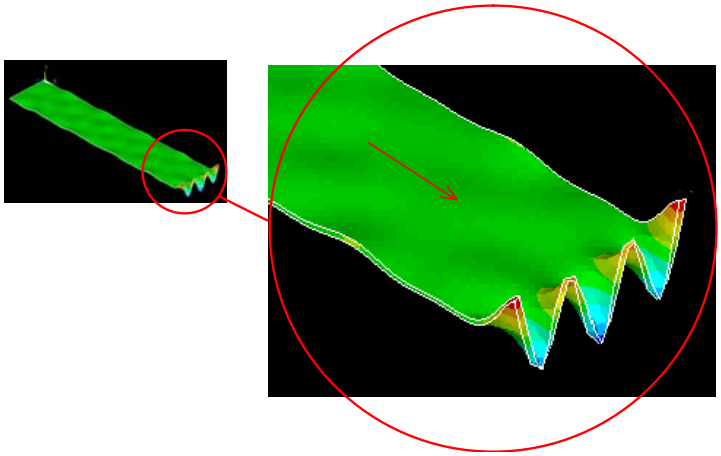

Fig. 5. A snapshot from computational modal analysis showing a standing vibration mode.

The effect of Reynolds number

Next we present the effect of Reynolds number on the plate vibration and on the organization of vortex shedding. One has to bear in mind that the development of the wake is not entirely determined by fluid mechanics and thus the Reynolds number is not the only relevant parameter affecting the vibration mode and details of vortex shedding. Basically, there are two ways to vary the Reynolds number in the present setup: changing the flow rate and changing the splitter plate tip thickness. Here only the flow rate is used as a parameter. Experiments are conducted to cover a range of Reynolds numbers starting from Re=4360 and extending up to Re=14800. Measurements at 76 velocity points are carried out, which results in steps of 140 units in Reynolds number.

First results are presented for vibration frequency as a function of the Reynolds number in Fig. 6. The vibration frequency (f_o) does not increase smoothly as the flow rate is increased, but changes with stepwise increments. The frequencies in the plot correspond to the dominating peak in the spectrum at given Reynolds number. At certain Reynolds numbers, several vibration frequencies are observed. However, the dominating peak typically has an order of magnitude higher power than that of the other peaks. The plateaus, i.e. ranges of rather constant f_o in the plot are referred to as frequency branches in the following. Typically there is a discontinuous jump between two branches as the flow rate exceeds a threshold value for the higher branch. Note that a moderate increase in the vibration frequency occurs also within the frequency branches. Some of the vibration branches are also labeled for more detailed discussion in the following.

Over most Reynolds numbers studied the plate responds at a single vibration frequency and the response in the flow is a well-ordered periodic streak pattern. Obviously, the frequency selection is not entirely based on fluid mechanics. If this were the case, a continuous increase in the vibration frequency would be expected. The stepwise increase can be explained by the VIV. Fig. 7 illustrates the same data as in Fig. 6, but as a variation of non-dimensional vibration frequency, the Strouhal number (St_o), which is here based on the vibration frequency (f_o) rather on vortex shedding frequency. As a function of Reynolds number St_o is confined between the values of 0.16 and 0.19

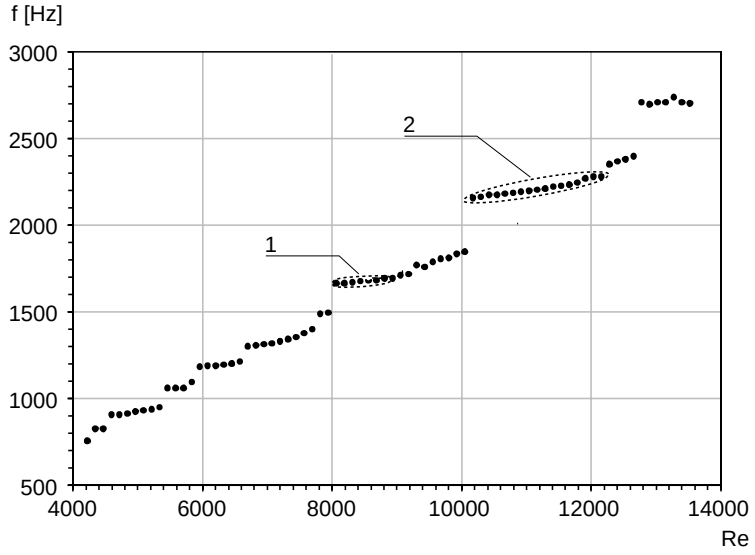

Fig. 6. Vibration frequency of the plate tip as a function of Reynolds number.

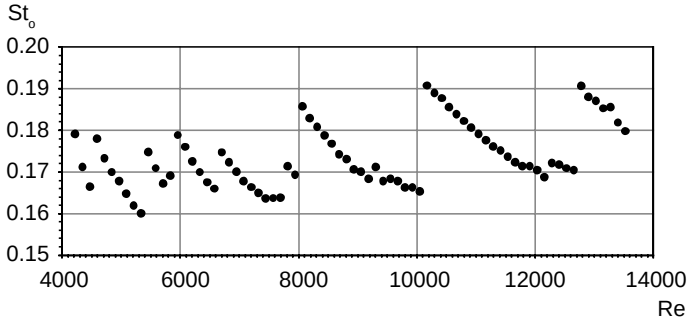

Fig. 7. Non-dimensional vibration frequency (St_o) as a function of the Reynolds number.

and forms a saw-tooth profile. This is a clear indication that both solid and fluid mechanics are involved. The plot can be explained as follows. Within a frequency branch, the vortex shedding frequency is tuned to a value amplified by the fluid-structure system. As soon as this frequency drifts out of the range sustained by the flow instability the VIV finds a new balance from the next frequency branch. This process is repeated over the entire Reynolds number range studied. The value for the fixed body cannot be determined at this high Reynolds number. However, the Reynolds numbers showing low vibration energy and small amplitude are located at the end of the vibration branches and are thus characterized by low Strouhal numbers between 0.16 and 0.17. Furthermore, reduced velocity of the system i.e. the inverse of the non-dimensional vibration frequency (St_o) defined as:

$$U_r = \frac{U_E}{f_o D} \qquad \text{Eq. 1}$$

is bound between U_r = 5.25… 6.25, which is known to be the range of highest amplitude response for circular cylinders. It is an interesting question why the response is confined to this narrow range. Obviously, tightly spaced natural frequencies allow a new vibration branch to emerge as soon as desynchronization in the former branch occurs.

Most branches show a well-organized and periodic pattern, which is a consequence of a highly regular vibration mode. The streaks in the mean flow field appear immediately as the jump in the vibration frequency occurs and the streak spacing remains constant over the entire branch. Figs. 8 and 9 illustrate the mean flow streak patterns and the corresponding vibration spectra from the branches 1 and 2, respectively. In addition, also two other examples with less regular vibration mode with Re numbers between the highly regular branches 1 and 2. The first example is measured at Re = 8190. One very clear peak appears in the spectrum. At this Reynolds number the streaks in the mean velocity field are highly periodic. As the Reynolds number is increased to Re = 8930, two

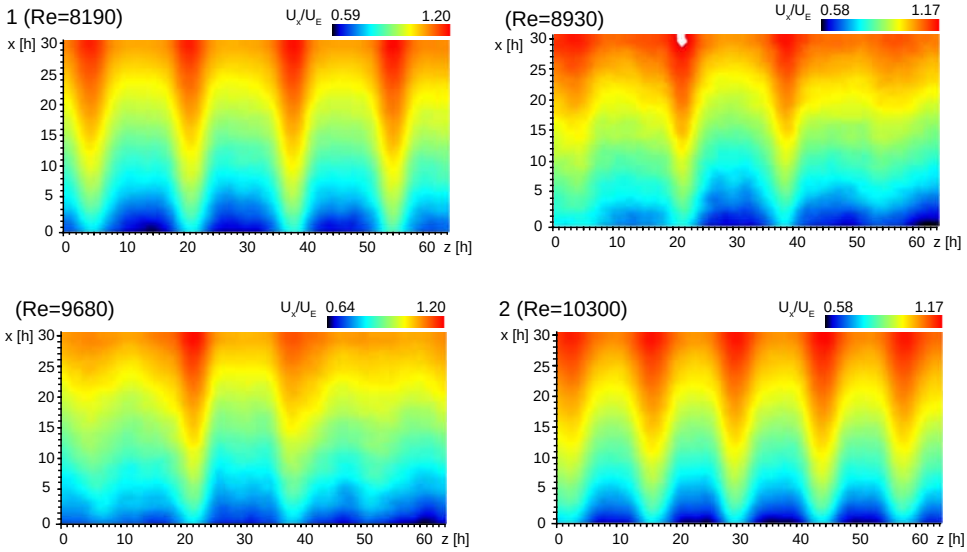

Fig. 8. Selected mean-velocity fields showing the effect of Reynolds number.

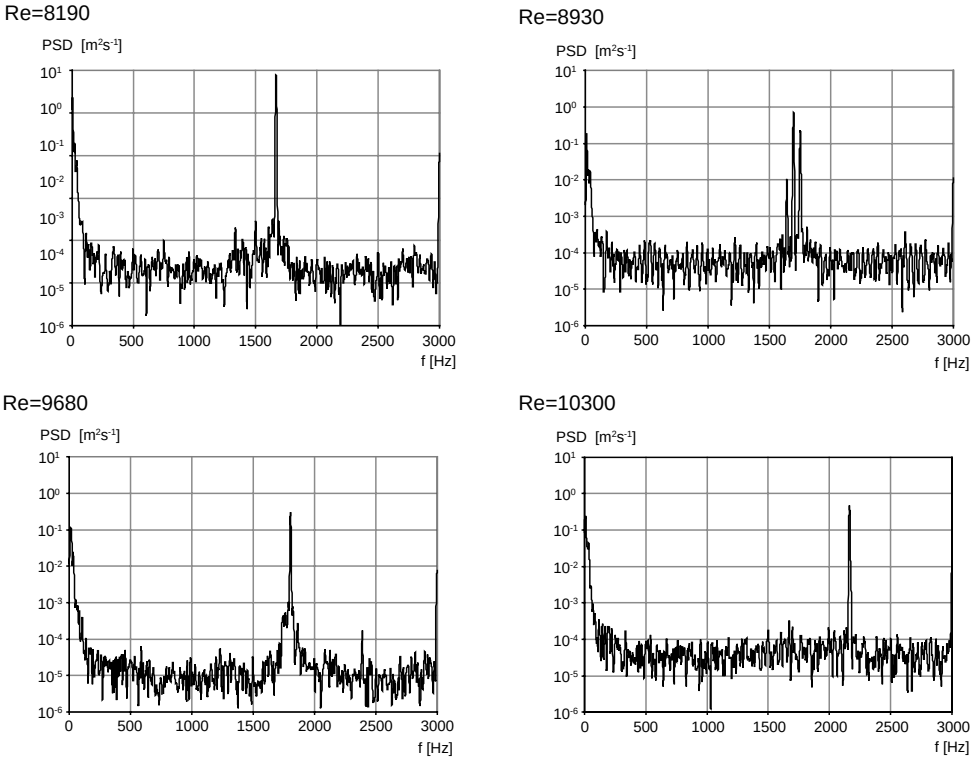

Fig. 9. Tip vibration spectra measured with HSDI corresponding to Reynolds numbers in Fig. 8.

additional peaks appear in the spectrum. All three peaks have rather high energy and the streak pattern being in transition from branch 1 to branch 2 is clearly less periodic. At this Reynolds number the response seems to be multi-modal as the frequency of the first peak from the left corresponds to the frequency at Re = 8190 and the last peak corresponds roughly to the frequency at the next example Re = 9680. This pattern is also not purely periodic and the magnitude of individual streaks varies. This is also observed from the spectra in which the peak has components from rather large band of frequencies. Finally, next branch is achieved at Re = 10300. Here the spectrum again shows only one narrow peak and the resulting flow pattern is highly periodic.

5. Conclusions

Particle Image Velocimetry (PIV) and High-Speed Digital Imaging (HSDI) are used to study Vortex-Induced Vibration (VIV) at the trailing edge a splitter plate. A splitter plate placed in a convergent channel vibrates in a well-defined mode, which is essentially characterized by a standing wave along the plate trailing edge. The imprint of the vibration mode can be clearly observed in the near wake as a periodic spanwise variation of streamwise mean velocity, which has been studied in Eloranta et al. (2005) in more detail. Present results show the development of the vibration mode as a function of Reynolds number. The vibration frequency does not increase smoothly with the Reynolds number, but in a stepwise fashion. In other words, only certain frequencies i.e. the natural frequencies of the system are amplified by the combined fluid-structure system. The vibration frequency locks-in to a rather constant value over a Reynolds number range in the vicinity of each amplified natural frequency. The characteristic vibration mode is initiated as soon as the synchronization of the vortex shedding frequency with a natural frequency of the system occurs. In the beginning of the vibration branch the amplitude of vibration increases. At some point the frequency starts to drift out of the range sustained by the VIV and the amplitude of vibration starts to decay. This development is reflected in the near-wake mean flow pattern too.

References

Castro I. P., Rogers P. (2002) Vortex shedding from tapered plates. *Exp Fluids* 33: 66 – 74.

Evangelinos C., Karniadakis G. (1999) Dynamics and flow structures in the turbulent wake of rigid and flexible cylinders subject to vortex-induced vibrations. *J Fluid Mech.* 400:91-124.

Eloranta H., Pärssinen T., Saarenrinne P. (2004) Analysis of fluid - structure interaction with PIV and LV; the case of a splitter plate in a converging channel. 12th International Symposium on Applications of Laser Techniques to Fluid Mechanics, Lisbon, Portugal, 12th – 15th July, 2004.

Eloranta H., Pärssinen T., Saarenrinne P. (2005) Fluid-structure interaction of a splitter plate in a convergent channel, *Exp Fluids* 39:841-855.

Eloranta H., Pärssinen T., Saarenrinne P. (2006) On the fluid-structure interaction of a splitter plate: vibration modes and Reynolds number effects. *Exp Fluids* in press.

Lucor D., Imas L., Karniadakis G.E. (2001) Vortex dislocations and force distribution of long flexible cylinders subjected to sheared flows. *J Fluids Struct* 15:641-650. DOI:10.1006/jfls.2000.0366.

Newman D., Karniadakis G.E. (1996) Simulations of flow over a flexible cable: A comparison of forced and flow-induced vibration. *J Fluids Struct* 10:439-453. DOI:10.1006/jfls.1996.0030.

Welch P.D. (1967) The Use of Fast Fourier Transform for the Estimation of Power Spectra: A Method Based on Time Averaging Over Short, Modified Periodograms. *IEEE Trans Audio Electroacoustics*, AU-15:70-73.

Willden R.H.J., Graham J.M.R. (2004) Multi-modal Vortex-Induced Vibrations of vertical riser pipe subject to a uniform current profile. *Eur J Mech B/Fluids* 23:209-218. DOI: 10.1016/j.euromechflu.2003.09.011.

Yamaguchi N, Sekiguchi T, Yokota K, Tsujimoto, Y (2000a) Flutter Limits and Behavior of a Flexible Thin Sheet in High-Speed Flow – I: Analytical Method for Prediction of the Sheet Behavior. *J Fluids Eng*, 122:65-73.

Yamaguchi N, Sekiguchi T, Yokota K, Tsujimoto, Y (2000b) Flutter Limits and Behavior of a Flexible Thin Sheet in High-Speed Flow – II: Experimental Results and Predicted Behaviors for Low Mass Ratios. *J Fluids Eng*, 122:74-83.